

Supporting Information

# **Self-Assembly Template Driven 3D Inverse Opal Microspheres Functionalized with Catalyst Nanoparticles Enabling a Highly Efficient Chemical Sensing Platform**

Tianshuang Wang,<sup>1</sup> Inci Can,<sup>2</sup> Sufang Zhang,<sup>1</sup> Junming He,<sup>1</sup> Peng Sun,<sup>\*,1</sup> Fangmeng Liu,<sup>1</sup> and Geyu Lu<sup>\*,1</sup>

1. State Key Laboratory on Integrated Optoelectronics, College of Electronic Science and Engineering, Jilin University, 2699 Qianjin Street, Changchun 130012, People's Republic of China.

2. Institute of Physical Chemistry, University of Tuebingen, Auf der Morgenstelle 15, 72076 Tuebingen, Germany.

Corresponding Authors:

E-mail: pengsun@jlu.edu.cn.

E-mail: lugu@jlu.edu.cn.

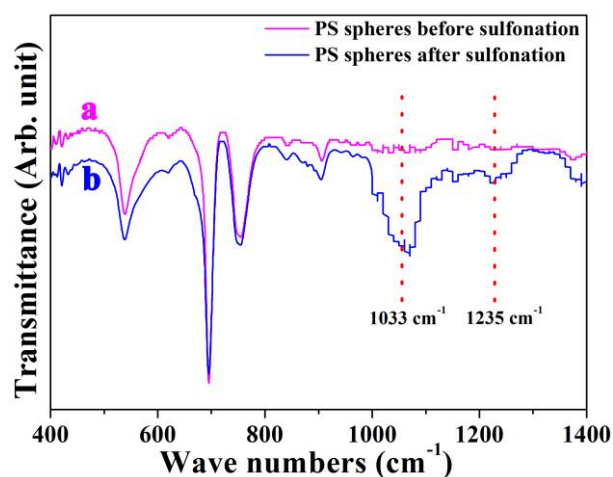


**Figure S1.** FT-IR spectra of (a) PS spheres before sulfonation and (b) PS spheres after sulfonation.

The powders of PS spheres before and after sulfonation were measured by using FT-IR spectroscopy. The FT-IR spectrum of PS spheres after sulfonation exhibited the peaks at about 1033 and 1235  $\text{cm}^{-1}$ , which were attributed to the symmetric and asymmetric stretching vibrations of sulfonic acid ( $\text{SO}_3\text{H}^+$ ) groups.<sup>1, 2</sup> Moreover, PS spheres before sulfonation did not have any distinct vibrational frequency in the 1000-1300  $\text{cm}^{-1}$  (**Figure S1**). Therefore, we could conclude that the S-PS spheres were obtained after sulfonation.

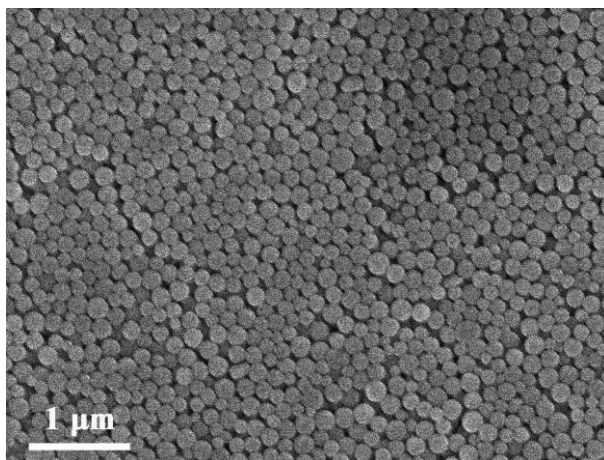


**Figure S2.** SEM image of S-PS spheres.

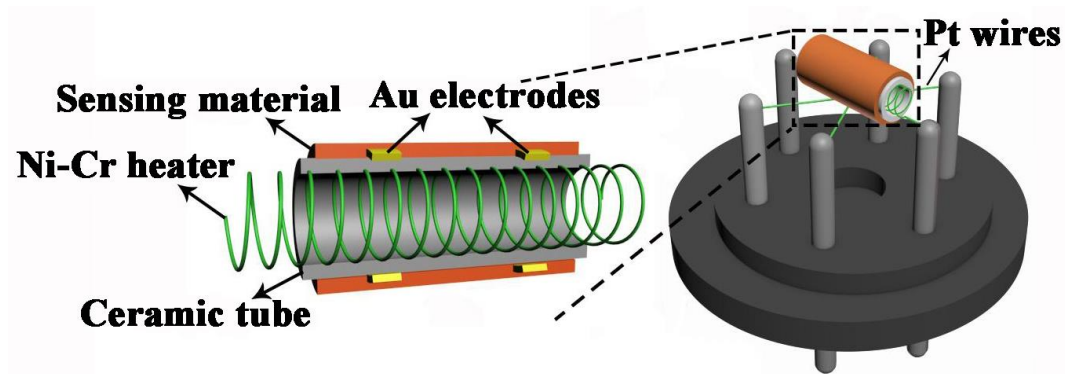


**Figure S3.** Schematic diagram of the gas sensor.

Detailed parameters of alumina tube: external diameter: 1.2 mm, internal diameter: 0.8 mm, and length: 4 mm; a couple of Au electrodes were previously printed on the end of the tube, and each electrode was connected with a pair of Pt wires.

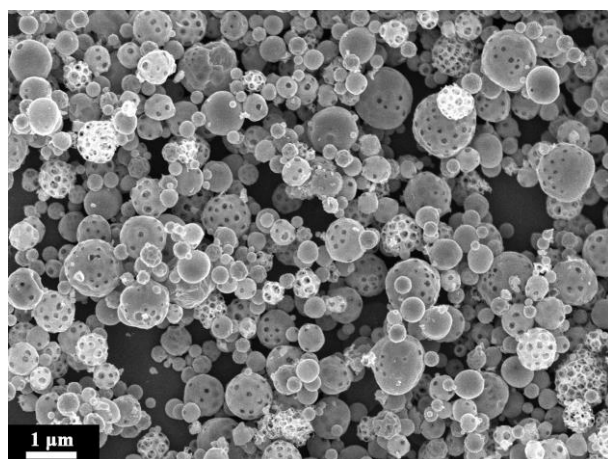


**Figure S4.** The SEM image of the precursor microspheres used to fabricate 3D-IO  $\text{In}_2\text{O}_3$  MSs (before annealed under an air atmosphere at a temperature of 600 °C for 3 h).

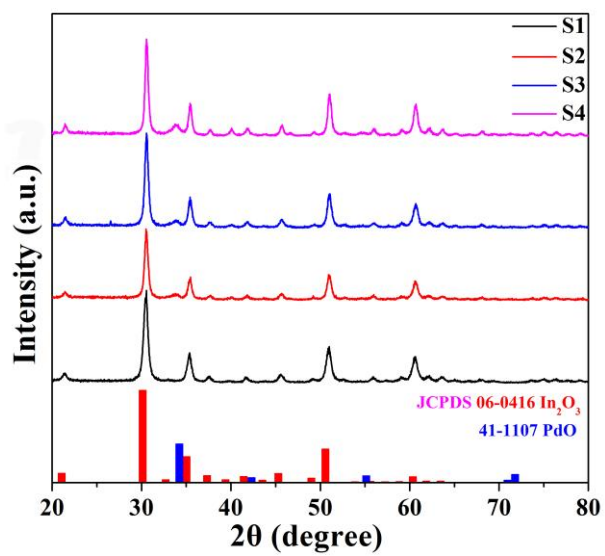


**Figure S5.** XRD patterns of the S1-S4 samples.

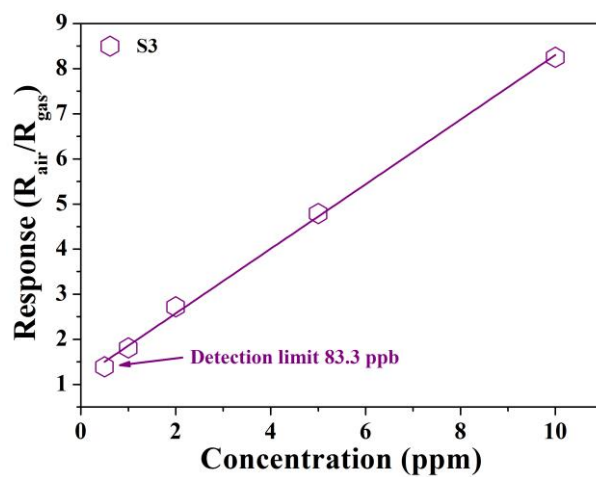


**Figure S6.** Linear approximation of the detection limit with S3 sensor.

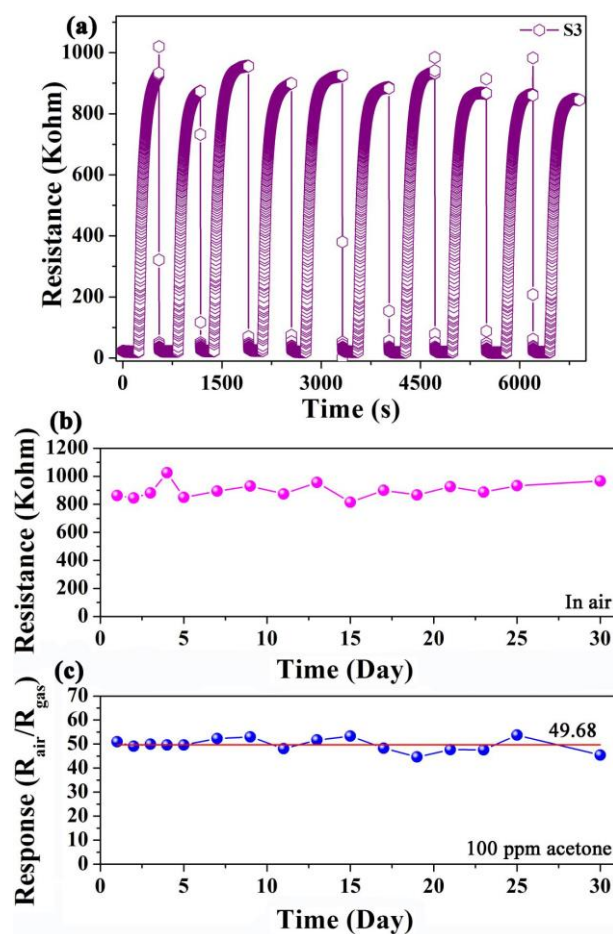


**Figure S7.** (a) The repeatability of the S3 sensor response at cyclic exposure to 100 ppm acetone at 250 °C; (b) and (c) Long-term stability of the S3 sensor measured at the operating temperature of 250 °C.

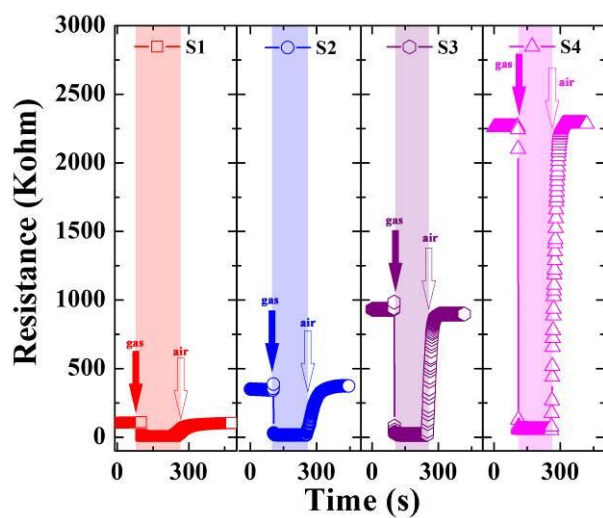


**Figure S8.** Dynamic resistance transitions of the S1-S4 sensors toward 100 ppm of acetone.

acetone at 250 °C.

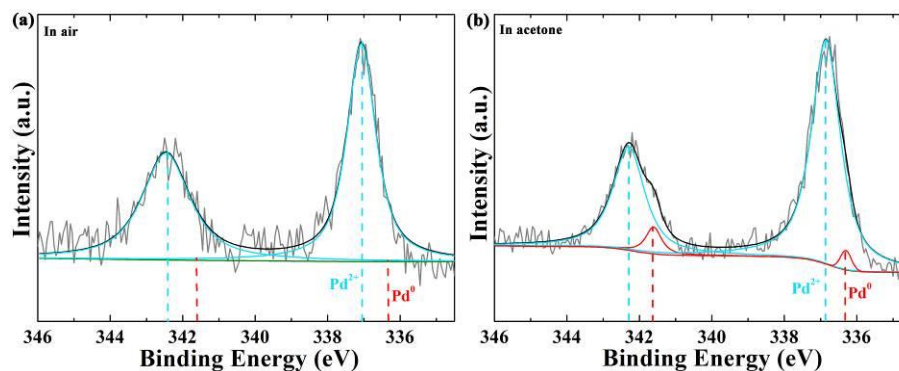


**Figure S9.** Ex situ XPS analysis spectra of 3D-IO PdO@In<sub>2</sub>O<sub>3</sub> MSs (S3 sample) in the vicinity of Pd 3d (a) in air and (b) in acetone after 10 cycles sensing measurement with 100 ppm of acetone at 250 °C.

We have carried out ex situ XPS analysis to elucidate the catalytic effect of PdO NPs. We noted that the PdO NPs are partially reduced to the Pd<sup>0</sup> state when exposed to 100 ppm of acetone, and the binding energy of Pd<sup>0</sup> state shifted to a higher energy compared to the standard binding energy after acetone sensing measurement, which can be attributed to the formation of Pd-In alloy.<sup>3</sup>

## REFERENCES

- (1) Fitzgerald, J. J.; Weiss, R. A.; Eisenberg, A.; Bailey, F.; Coulombic Interactions in Macromolecular Systems. Washington DC: American Chemical Society. **1980**, 35.
- (2) Lei, H.; Bu, N. J.; Chen, R. L.; Hao, P.; Neng, S.; Tu, X. F.; Yuen, K.; Chemical Mechanical Polishing of Hard Disk Substrate with  $\alpha$ -Alumina-g-Polystyrene Sulfonic Acid Composite Abrasive. Thin Solid Films. **2010**, 518, 3792-3796.
- (3) Rui, N.; Wang, Z. Y.; Sun, K. H.; Ye, J. Y.; Ge, Q. F.; Liu, C.-J.; CO<sub>2</sub> Hydrogenation to Methanol Over Pd/In<sub>2</sub>O<sub>3</sub>: Effects of Pd and Oxygen Vacancy. Appl. Catal. B-Environ. **2017**, 218, 488-497.